Pharmaceutical Research, Vol. 26, No. 2, February 2009 (© 2008)
DOI: 10.1007/s11095-008-9754-5

Research Paper

Blocking Effect of an Immuno-Suppressive Agent, Cynarin, on CD28 of T-Cell Receptor

Guo-Chung Dong,[2,4] Ping-Hsien Chuang,[1,2] Kai-chun Chang,[2] Pey-shynan Jan,[1] Pei-Ing Hwang,[2] Huan-Bin Wu,[2] Myunggi Yi,[3] Huan-Xiang Zhou,[3] and Hueih Min Chen[1,2,5]

Received August 24, 2008; accepted October 9, 2008; published online November 7, 2008

Purpose: Cynarin, a potential immunosuppressant that blocks the interaction between the CD28 of T-cell receptor and CD80 of antigen presenting cells, was found in *Echinacea purpurea* by a new pharmaceutical screening method: After Flowing Through Immobilized Receptor (AFTIR; Dong *et al.*, J Med Chem, 49: 1845-1854, 2006). This *Echinacea* component is the first small molecule that is able to specifically block "signal 2" of T-cell activation.
Methods: In this study, we used the AFTIR method to further confirm that cynarin effectively blocked the binding between CD80 of B-cells and CD28 of T-cells, and provide details of its mechanism of action.
Results: The experimental results showed that cynarin blocked about 87% of the CD28-dependent "signal 2" pathway of T-cell activation under the condition of one to one ratio of T-cell and B-cell *in vitro*. Theoretical structure modeling showed that cynarin binds to the "G-pocket" of CD28 (Evans *et al.*, Nat Immunol, 6:271-279, 2005), and thus interrupts the site of interaction between CD28 and CD80.
Conclusions: These results confirm both that AFTIR is a promising method for screening selective active compounds from herbal medicine and that cynarin has great potential as an immuno-suppressive agent.

KEY WORDS: blocking efficiency; cynarin; CD28; immuno-suppression; T-cell receptor.

INTRODUCTION

Resting T-cells are stimulated to initiate immune activity in response to specific external stimuli, such as by the approach of antigen-presenting cells (APCs). After making contact with an APC, resting T-cells are activated *via* the so-called "signal 1" and "signal 2" pathways (1–3). The "signal 1" pathway is initiated by a binding interaction between surface-presented antigen and the major histocompatibility complex (MHC) present on the cell surface of APC cells, and the T-cell receptor (TCR) of T-cells. Signal 1 only induces a partial T-cell response. In addition, there is a second signal, "signal 2", part of a co-stimulatory pathway for T-cells that is required for their full activation, which is induced by the binding between CD80 (also known as B7-1) of APC cells and CD28 (4) of T-cells *in vivo*. Following CD80 binding to CD28, additional cell surface molecules are induced in both APC cell and T-cells: CD86 (also known as B7-2) in APC cells and the CTLA-4 receptor of T-cells. The T-cell response from CD86 binding to CTLA-4 is inhibitory (negative immune response), resulting in a balance with the "positive" immune responses *via* binding between CD80 and CD28. To maintain T-cells in a healthy condition requires a balance of both "positive" and "negative" immune responses. Imbalanced bindings between CD28 and CD80 and between CTLA4 and CD86 responses, both "over-active" and "under-active" immune responses are pathological. There are many autoimmune disease examples of "over-active" immune responses.

Compounds such as FK506 (tacrolimus), which penetrates the cell membrane and intracellularly shuts down particular pathways including signal 1, are currently being investigated or used clinically as immunosuppressive agents (5,6). While FK506 is a useful immuno-suppressive agent with significant effects on T-cells for example, in inhibition of transplantation rejection, it has severe side effects since it shuts down many pathways in the cell. This indiscriminate behavior also affects cells in other organs. For example, the calcium ion pathway in cells is altered by FK506 due to its effects on calcineurin, which may subsequently lead to the disease of osteoporosis (lack of calcium in bone). Therefore, recent efforts to find new immuno-suppressive drugs have focused on cell membrane receptor's antibodies (for example anti-CD28 antibody, a non-mitogenic antibody being considered as outside T-cell blocker), which can efficiently block

[1] Nano BioSystem Technology Division, National Nano Device Laboratories, Hsinchu, 300, Taiwan.
[2] Agricultural Biotechnology Research Center, Academia Sinica, Taipei, 115, Taiwan.
[3] Institute of Molecular Biophysics, Florida State University, Tallahassee, FL 32306, USA.
[4] Department of Chemistry, National Chung Hsing University, Taichung, 402, Taiwan.
[5] To whom correspondence should be addressed. (e-mail: hmchen@ndl.org.tw)

ABBREVIATIONS: AFTIR, after flowing through immobilized receptor; APC, antigen-presenting cell; MHC, major-histocompatibility-complex; TCR, T-cell receptor.

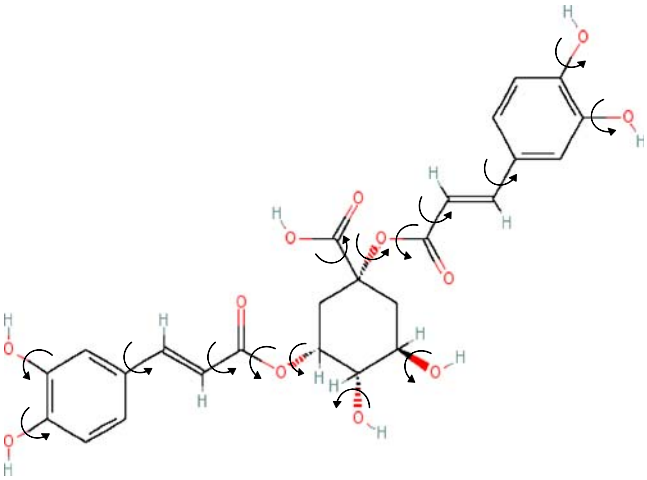

Fig. 1. Structure of cynarin. Cynarin (1,3-dicaffeoylquinic acid) structure was confirmed by mass spectroscopy and H^1 NMR and C^{13} NMR[5].

receptors but not affect other pathways inside cells. However, using antibodies as drugs has many drawbacks including their fragile nature (protease and peptidase digestion limits oral availability and half-life) and poor stability (loss of 3-D structure). Also, unlike small molecules, which mimic metabolites in the body, the large antibodies might induce other immune system problems and therefore reduce their therapeutic utility.

In this study, the small organic compound, cynarin (see Fig. 1), previously isolated from the north American herb *Echinacea purpurea* with our recently established screening method: After Flowing Through Immobilized Receptor (AFTIR; see Fig. 2) (7) was further investigated. A detailed understanding of the mode and types of binding of cynarin to T-cell receptors is essential for further development of this potentially new "mild" immuno-suppressive agent.

MATERIALS AND METHODS

Chemicals and Reagents. Silica gel 60 M (0.040–0.063 mm) for chromatographic column packing was purchased from Macherey-Nagel (Düren, Germany). Elution solvents *n*-hexane, ethyl acetate and methanol (MeOH, ChromAB grade, code no. 3041-68) were purchased from Mallinckrodt Baker Inc. (Paris, KY). Silica gel 60 F_{254} thin layer chromatography (TLC) 200 μm plates were purchased from Merck (Darmstadt, Germany). Trifluoroacetic acid (TFA 99% purity; Fluka, Switzerland) was used for eluent pH adjustment. The cynarin reference standard (Batch No. CHI20041218, 98.4%) was obtained from Fleton Reference Substance Co., Ltd. (Chengdu, People's Republic of China). All other chemicals used were of analytical or chromatographic grade.

Cell Lines, Media and Antibodies. Jurkat human acute T-cell leukemia and Raji human B lymphocyte lines were obtained from the Bioresource Collection and Research

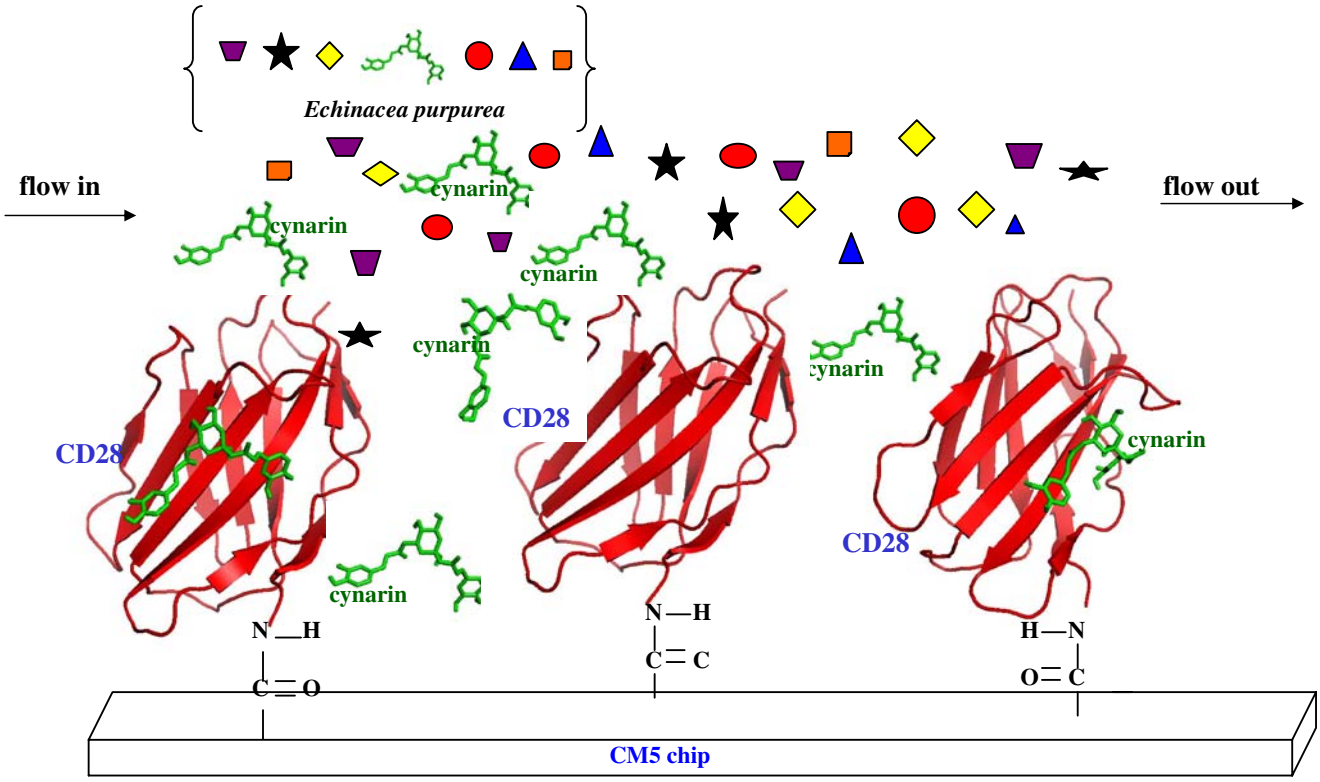

Fig. 2. AFTIR scheme. The compound cynarin was discovered in *Echinacea* extract by the AFTIR method. This schematic diagram shows the immobilization of CD28 (extra-cellular part) in the chip. Many components from the extract of *Echinacea purpurea*, including cynarin, are indicated by different symbols flowing across the immobilized CD28. Subsequently, only cynarin is bound to the specific binding site of CD28, and other components are washed off the chip.

Center (BCRC: HsinChu, Taiwan). RPMI-1640 medium was purchased from HyClone (Logan, UT). Fetal bovine serum (FBS) was purchased from Biological Industries (Haemek, Israel). Penicillin–Streptomycin–Neomycin (PSN) Antibiotic Mixture was purchased from Gibco BRL (Rockville, MD). ELISA kits for human IL-2 were obtained from R&D Systems (Minneapolis, MN). Anti-human CD28 antibody and anti-human CD3 antibody were purchased from BioLegend (San Diego, CA). 3-[4,5-Dimethylthiazol-2-yl]-2,5-diphenyltetrazolium bromide (MTT) was purchased from Sigma (St. Louis, MO). Water used in this study was deionized and distilled. Anti-IL-2 mAb was supplied by R&D Systems (Minneapolis, MN).

Purification of Cynarin. Cynarin was purified from *Echinacea purpurea* extracts on a silica gel open column with serial elution buffers of 1 L of 100% *n*-hexane, 1 L of 100% ethyl acetate (EA), 3 L of 50% MeOH in EA, 3 L of 75% MeOH in EA and 3 L of 100% MeOH. 200 mL of eluate with each elution buffer was collected. After removal of solvent and re-dissolution of eluted extract in water, the composition of collected fractions was analyzed by HPLC under the same condition as used for *Echinacea* crude extract. A typical HPLC profile (absorbance at 254 nm) for cynarin fraction and for *Echinacea* crude extract are shown in Fig. 8A, (a) and (b), respectively. Composition of collected fractions was also monitored by TLC using Silica gel 60 F_{254} plate in an EA: isopropanol: H_2O (8:5:3, *v*/*v*/*v*) mobile phase.

After HPLC analysis with DAD detector had determined the cynarin fraction, the UV spectrum was recorded over the whole elution duration (0–60 min.; see Fig. 8B). The fraction marked by "T" shown in Fig. 8A, (a) was collected at a retention time of 32.612 min, and the UV spectrum is shown in Fig. 8B (black). For comparison, a UV spectrum of crude extract is overlaid in Fig. 8B (blue). The results show that the UV intensity of pure fraction including cynarin is much higher than that of crude extract (note the different intensity scales). The absorption peak shifted from 338 nm (crude extract) to 330 nm (cynarin pure fraction).

Stimulation of T-Cells. Jurkat T-cells were maintained in a humidified atmosphere of 5% CO_2/95% air at 37°C in RPMI-1640 medium including penicillin, streptomycin and 10% heat-inactivated FBS. Two modes of T-cell stimulation were used for the present experiments: Route 1 (R1): anti-CD3 and anti-CD28, and Route 2 (R2): anti-CD3 and Raji B-cells. (1) R1: signal 1 and signal 2 were stimulated *via* addition of anti-CD3 and anti-CD28, respectively. Flat-bottom 96-well plates were coated with 10 μg/mL of anti-CD3 for 24 h at 4°C. Wells including anti-CD3 were then washed twice with phosphate-buffered saline (PBS) to remove unbound anti-CD3. Jurkat T-cells (200 μL, 2×10^6 cells/mL) with or without cynarin (PBS buffer only; control group) were then added to the wells. Cells were activated by anti-CD3 in wells for 15 min (signal 1 stimulation). Consequently, anti-CD28 (1 μg/mL) was then added into the wells (for signal 2 stimulation) for 24 h at 37°C. IL-2 release from stimulated T-cells (100 μL) was then measured by enzyme-linked immunosorbent assay (ELISA; see section below for detail). (2) R2: similar procedures as shown for R1 above, 100 μL Jurkat T-cells (2×10^6 cells/mL) with or without cynarin in PBS were pre-incubated with anti-CD3 (50 ng/mL) for 15 min and then 100 μL Raji cells (2×10^6 cells/mL) were added to wells for 24 h at 37°C. IL-2 release from 100 μL of co-cultured T-cells was again determined by ELISA.

IL-2 ELISA. A 96-well flat-bottom plate was coated with anti-IL-2 mAb (100 μL at 4 μg/mL) in PBS (pH 7.3) at room temperature overnight. The plate was washed three times with 300 μL of PBS containing 0.05% Tween 20 (PBS-T) and was incubated for more than 1 h with a blocking solution containing 1% bovine serum albumin in PBS. After plates were washed again with PBS-T, 100 μL of testing sample (T-cell incubation medium) and 100 μL of biotinylated anti-IL-2 detection antibodies (400 ng/mL) were added and incubated for 2 h at room temperature. Finally, 100 μL of streptavidin horseradish peroxidase (1/2,000 dilution of a 1.25 mg/mL solution) and 100 μL of substrate solution containing H_2O_2 and tetramethylbenzidine (1:1 by volume) were added for another 20 min in the dark at room temperature. The reaction was terminated by the addition of 50 μL stop solution (1 M H_2SO_4). The optical density of each well at 450 nm was determined using a microplate reader. The amount of IL-2 released from T-cells was normalized by relative percentage (i.e. an IL-2 quantity, 1,200 pg/μl, is defined as 100%).

MTT Colorimetric Assay. The cytotoxicity of cynarin treatment of T-cells was measured by MTT colorimetric assay. 100 μL Jurkat cells (5×10^5 cells/mL) were incubated with different concentrations of cynarin for 24 h at 37°C. The cell solution was then centrifuged at 200×*g* for 10 min and the supernatant removed. 200 μL of MTT (0.5 mg/mL in culture medium) was then added and the cell solution was incubated again for 4 h at 37°C. 200 μL of DMSO lysis buffer was added into the cell medium and the concentration of dissolved MTT crystals was measured by plate reader (Dynatech, Chantilly, VA) at 560 nm. The survival rate (%) was determined as follows: OD_{560nm} of tested sample (cells with cynarin)/ OD_{560nm} of control (cells without cynarin)×100%.

Molecular Modeling and Docking. Cynarin (1,3-dicaffeoylquinic acid) was coordinated (PRODRG2) (8) based on AutoDockTools (9), All hydrogen and flexible bonding of cynarin shown in Fig. 1 were arranged to render Gasteiger charge assignment. Crystal structure of CD28 was obtained from Protein Data Bank (PDB/RCSB, 1YJD). The analysis of automated docking including those parameters for global docking was carried out (9): an initial population of random individuals with a population size of 250 individuals was done and a maximum number of 1×10^7 energy evaluations plus 100 docking runs were executed. The rest of the parameters were set as default values. The grid maps were generated with 94×126×110 points (grid-point spacing at 0.375 Å) by using AutoGrid for CD28. To cluster the docked complex conformations (CD28 with cynarin) according to their docked locations, the center-of-mass for each of the predicted cynarin conformations was computed. Using each ligand conformation as a reference, the complex conformations with distance less than 3 Å from its center-of-mass to the center-of-mass of the reference were grouped into the same cluster. The clustering is started with the reference of the conformation

which had been surveyed by the lowest docked energy. A ligand was assigned to a cluster once and was not used repeatedly. The process was repeatedly boosted until all conformations were stimulated in the same cluster. For local docking, the grid maps, centered on the G-pocket binding site, were produced with 64×60×60 points and a grid-point spacing at 0.375 Å. The docking parameters were set as following: a population size of 250 individuals; a maximum number of 2.5×10^6 energy evaluations and 50 docking runs. For both global and local dockings, the clustering tolerance for the root-mean-square positional deviation was set at 1.5 Å. The distance of center of mass between ligand and protein was measured using VMD program (10) and the results of docking were presented using PYMOL software (11).

To identify the amino acids in CD28 which may interact with cynarin through hydrogen bonding, the cluster consisting of eleven CD28–cynarin conformations predicted with the lowest docked energies (mean kilocalorie per mole) from local docking procedure was closely examined.

RESULTS

Cynarin Inhibition of both Signal 1 and Signal 2-Stimulated IL-2 Secretion. Jurkat T-cells (1×10^6 cells/mL) were simultaneously activated *via* both signal 1 and signal 2 by (1) R1: anti-CD3 (signal 1) and anti-CD28 (signal 2) or (2) R2: anti-CD3 (signal 1) and Raji cells (B-cells expressing cell surface receptor, CD80, to activate signal 2 *via* binding with CD28). When Jurkat T-cells are activated, they secrete increased amounts of IL-2, while, if inhibition occurs, the secretion of IL-2 by T-cells is reduced. The inhibition by cynarin of activated Jurkat T-cells secretion of IL-2 was investigated as a function of concentration (see Fig. 3). The quantity of IL-2 was measured by ELISA and was normalized to 100% at zero cynarin concentration. The IC_{50} of cynarin was 823 μg/mL on R1 (filled square symbols) and 512 μg/mL for R2 (open circles). MTT cell survival assay confirmed there was no cytotoxic effect from cynarin on Jurkat T-cells within the concentration used (up to 1,000 μg/mL; filled triangles).

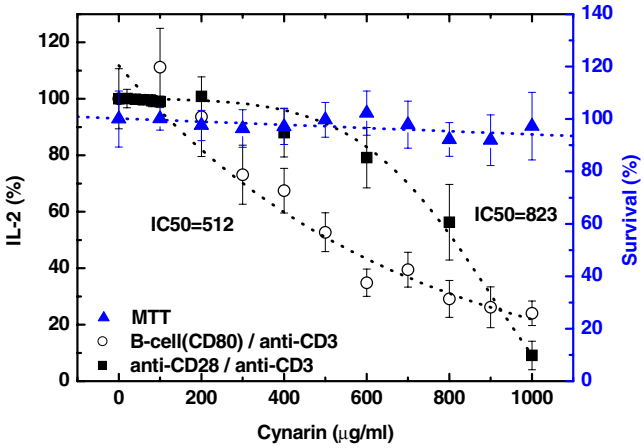

Fig. 3. IC_{50} on co-stimulated (signal 1+signal 2) of T-cell activation and cytotoxicity of cynarin. The reductions of IL-2 production by T-cells as a function of concentration of cynarin was plotted by route 1 (R1) (anti-CD3+anti-CD28; *filled squares*) and route 2 (R2) (anti-CD3+B-cell; curve represented by *open circles*). There was little cytotoxicity seen in T-cells at all concentrations of cynarin used, up to 1,000 μg/mL (MTT assay; represented by *filled triangles*). The experiments were repeated four times and the average value and error in average were shown.

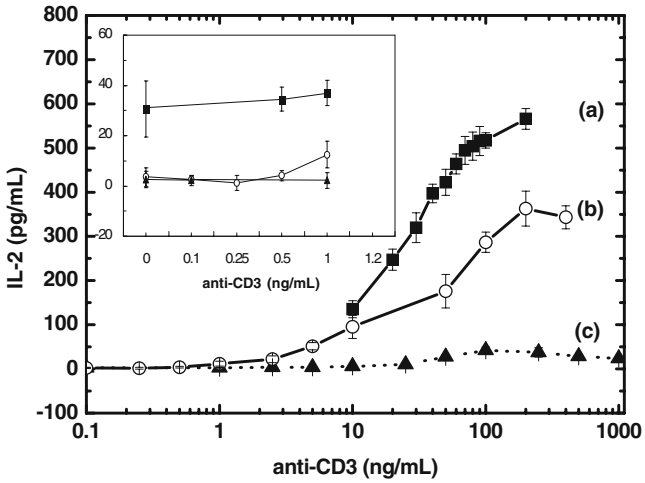

Fig. 4. Cynarin inhibition of T-cell signal 2-stimulated IL-2 production. Signal 1 stimulation of T-cell immune response was initiated by the Addition of anti-CD3 antibody and signal 2 was produced by the co-culture of CD28-riched Jurkat cells with CD80-riched Raji cells. At the fixed signal 2 (co-culture of Jurkat cells with Raji cells), the quantity of IL-2 is gradually increased by the addition of anti-CD3 antibody (curve (a)). With the addition of cynarin (500 μg/mL), the production of IL-2 was reduced as shown in curve (b). Without the addition of Raji cells, the IL-2 was not produced (see curve(c)). The inset panels indicate the production of IL-2 is lower at low concentration of anti-CD3 antibody. The experiments were repeated four times and the average value and error in average were shown.

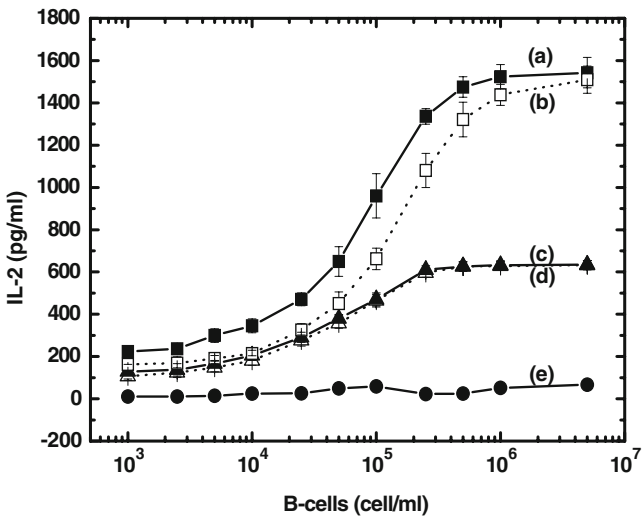

Fig. 5. Cynarin inhibition of T-cell signal 1-stimulated IL-2 production. Jurkat T-cells (1×10^6 cells/mL) were co-cultured with different cell densities of Raji cells (1×10^3 to 5×10^6 cells/mL). Anti-CD3 antibody was added at 100 ng/mL (curve (a) without cynarin and curve (b) with 500 μg/mL cynarin) and at 50 ng/mL (curve (c) without cynarin and curve (d) with 500 μg/mL cynarin). T-cell IL-2 production without anti-CD3 antibody was shown in curve (e). The experiments were repeated four times and the average value and error in average were shown.

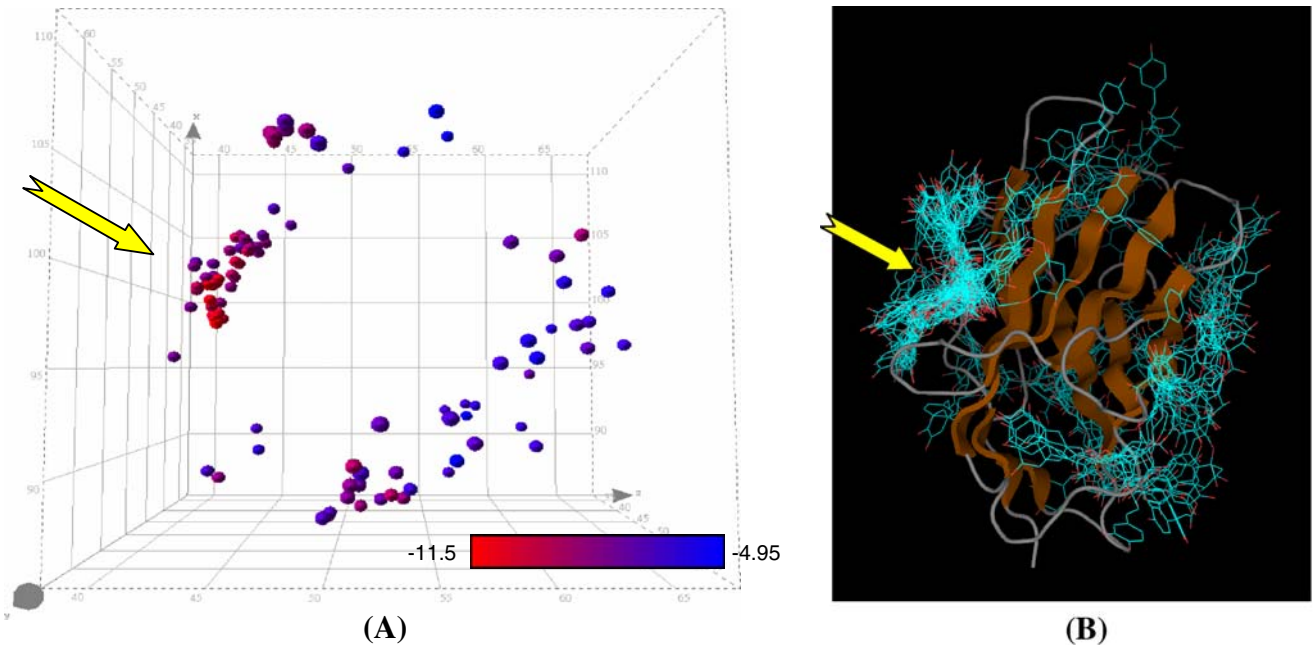

Fig. 6. G-pocket of CD28 appeared to be the most probable binding site for cynarin. Spatial locations of cynarin on CD28 were predicted with 100 runs of global docking analysis using AutoDock. **A** 3-D structure of CD28 with 100 superimposed cynarin predicted to be docked onto the receptor. The *yellow arrow* indicates the location of G-pocket. The *spheres* indicate the center-of-mass of a cynarin molecule. The calculated docked energies were presented with a red-to-blue gradient. *Red* indicated the lowest docked energy (i.e. −11.5 kcal/mol in this study and suggesting the most probable conformation) while *blue* shows the highest (i.e. −4.95 kcal/mol). **B** A 3D scatter plot to show the binding location on CD28 for each of the 100 predicted cynarin binding. The *yellow arrow* indicates the location of G-pocket. The majority of the predicted cynarin bindings were clustered at the G-pocket of CD28 with relatively lower docked energies than the rest.

Cynarin Inhibition of Signal 2-Stimulated IL-2 Secretion. Activation of T-cells in nature requires both signal 1 and signal 2. In this experiment, signal 2 was firstly initiated through the co-culture of CD28-enriched Jurkat T-cells (1×10^6 cells/mL) with CD80-enriched Raji B-cells (1×10^6 cells/mL). Afterwards, signal 1-stimulation of T-cells was gradually enhanced by the addition of anti-CD3 antibody. Without the addition of cynarin, the IL-2 level increased as the concentration of anti-CD3 antibody was increased (Fig. 4 (a)). With the addition of cynarin (500 μg/mL), the production of IL-2 was reduced as shown in Fig. 4 (b). Without the addition of Raji B-cells, there was no production of IL-2 as the concentration of anti-CD3 antibody was increased (see Fig. 4 (c)). Without the addition of anti-CD3

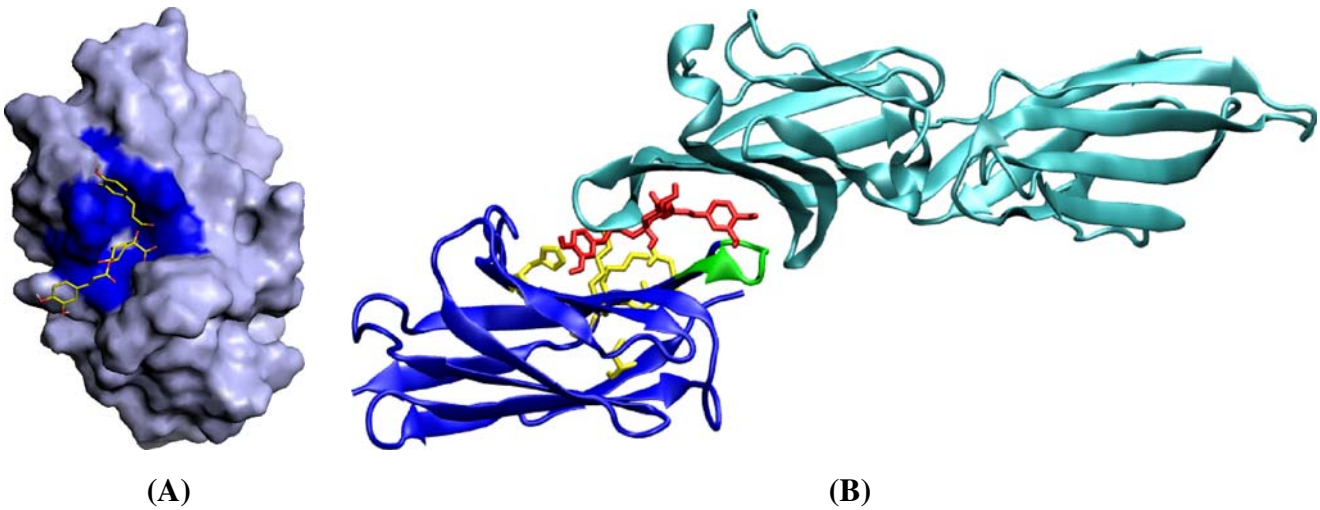

Fig. 7. Computer simulation for the 3-D structure of a cynarin bound CD28. 3D structure of CD28–cynarin complex predicted with the lowest docked energy was modeled by using PyMol[9]. **A** The interaction of cynarin with CD28 is shown by solid surface. The G-pocket of CD28 was colored in *blue*. The bounded cynarin to CD28 was presented in *sticks*. **B** Computer autodock simulation of the blocking effect of cynarin (*middle part in red*) between CD28 (*lower part in blue*; possible amino acids interacting with cynarin are indicated in *yellow*; the *green* shows the loop of "MYPPPY"[12]) and CD80 (*upper part in light blue*; 3D structure of CD80 was cited from PDB/RCSB: 1DR9).

antibody (see inset panel; zero concentration of anti-CD3 antibody), the quantity of IL-2 is about 30.5 pg/mL (where the production of IL-2 is purely due to signal 2). Under this condition, cynarin inhibits about 87.4% of signal 2-stimulated IL-2 production (3.8 pg/mL of IL-2 is produced at zero concentration of anti-CD3 antibody).

Cynarin did not Inhibit Signal 1-Stimulated IL-2 Secretion. Activation of Jurkat T-cells requires the binding of anti-CD3 antibody to TCR/CD3 (signal 1) and CD80 to CD28 (signal 2). Jurkat T-cells (1×10^6 cells/mL) were incubated with different concentrations (1×10^3 to 5×10^6 cells/mL) of Raji B-cells to see the effect of cynarin on signal 1 of T-cells in the presence of two concentrations of anti-CD3 antibody (Fig. 5 (a) and (b): 100 ng/mL anti-CD3, and Fig. 5 (c) and (d): 50 ng/mL anti-CD3). In Fig. 5, curves (b) and (d) were generated in the presence of 500 μg/mL cynarin, curves (a) and (c) show the IL-2 production with no added cynarin. The results showed that cynarin showed only minimal inhibition of IL-2 production at different concentrations of anti-CD3 antibody. Curve (e) of Fig. 5 shows the absence of an immune response when no anti-CD3 was added.

Binding between Cynarin and CD28. The binding site of CD28 for cynarin was preliminarily predicted by grid calculations on only CD28's extra-cellular domain (PDB/RCSB code 1YJD) by using AutoDock Tools (9). Afterwards, we further based on the method reported by Hetenyi and Spoel (12) to analyze the global docking of CD28–cynarin complex with at least 100 runs. The results show that a group of 46 conformations bind intensely to a particular area of CD28 and the rest of 54 conformations are distributed over various other sites (mainly grouping into two sites) on CD28 (see Fig. 6A). Further investigation was shown in Fig. 6B indicating 100 binding complexes were intensely grouped into three clusters. According to the relative spatial distances between the center-of-mass of two putative bound cynarin, 44 out of 46 cynarin molecules were bounded to the so-called G-pocket area (13) of CD28. Based on these observations, further binding details of cynarin molecule with specific amino acids of CD28 (see Fig. 7A) were done using "local docking" *via* Autodock program. The results preliminarily indicate that about nine amino acid candidates were possibly found to form hydrogen bonding with cynarin: i.e. Lys2, His38, Ser43, Cys94, Asn106, Asn107, Lys109, Ser110 and Asn111. Among these candidates, His38, Asn107, Lys109, and Ser110 are located in the G-pocket area of CD28. We predict that the Serine at position 110 may be the most possible to form hydrogen bond with cynarin in all the simulated binding modes.

DISCUSSION

The method of AFTIR previously reported (7) has been further demonstrated here to be a targetable and efficient screening technique. Using AFTIR, we identified an immunosuppressive compound, cynarin, which can block CD28 receptor of T-cells from binding with ligands such as CD80 of B-cells. The computer simulation about the possible block effect of cynarin between CD28 and CD80 was predicted and shown in Fig. 7B.

We further investigated the binding of cynarin to the CD28 of T-cell receptor to confirm its effectiveness as an antagonist of the CD28/CD80 interaction and to ascertain its potential as an immunosuppressive agent. Its high efficacy blockade of the signal 2 pathway mediated through CD28 of T-cells was confirmed. Cynarin binds more strongly to CD28 than CD80 does, and has no significant binding to other T-cell receptors such as CD154, CD86 and CD40 (unpublished results). This implies that cynarin may have few side effects in the body and could be a good candidate for future therapeutic drug development as an immunosuppressive agent, an outside T-cell blocker.

The cynarin inhibition of T-cell IL-2 release is not strong, since IC_{50} is about 512 μM for combined signal 1 and signal 2

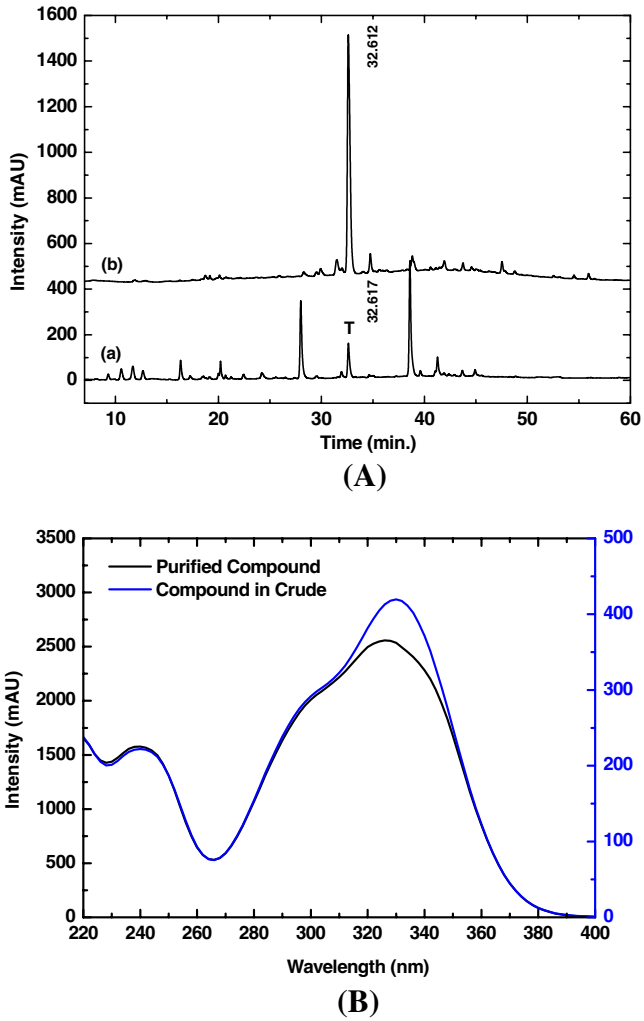

Fig. 8. HPLC profiling of cynarin fraction. Cynarin was purified from *Echinacea* extracts by using silica gel open column as shown in **A** curve (*a*). The absorption wavelength is at 254 nm. For comparison, the crude extract HPLC profile of *Echinacea* was shown in **A** curve (*b*) where T indicates the target to be isolated. The UV–VIS (220 to 400 nm) spectra of purified cynarin and crude extract at retention time of 32.612 min are shown in **B** curves (*black*) and (*blue*), respectively. Note the separate spectral intensities were indicated for purified cynarin (curve in *black*) and crude extract (curve in *blue*).

induced IL-2 release. When cynarin blocks signal 2 of T-cell only (i.e., not blocking signal 1) there is about 87% reduction of signal 2 of T-cell activation. Cynarin could be a mild immunosuppressive compound with fewer side effects. *In vivo*, immune responses occur in response to the presentation of foreign antigens to T-cells. The T-cell activation is moderated by the inhibition from CTLA-4 activation. The activation of both positive responses (such as from CD80 binding to CD28) and negative responses produces a balanced immune response. For patients with autoimmune diseases, the balance is shifted towards more positive immune responses causing an immune hyper-reaction. Thus, cynarin, which blocks signal 2 only, could be used to suppress patients' immune hyper-reaction. The mild immunosuppressive agent like cynarin might be suitable for children who suffer allergenic diseases. Furthermore, cynarin is one of main components in the American herb, *Echinacea purpurea* (see Fig. 8A, curve b). As shown in the section of cynarin purification, the yield of this compound from *Echinacea* would be sufficient in quantity and practically useful in the future clinical applications: i.e. Cynarin has satisfied the first requirement of "enough quantity" for later drug development as a mild immunosuppressive agent.

Based on a preliminary computer simulation, we predict that the cynarin binding site is located in the "G-pocket" of CD28 and that when bound, it interacts with the nearby "MYPPPY" Loop (14) (see Fig. 7B, green part). This is probably an area that CD80 binds to. If CD80 is weakly bounded to the CD28 with 1.11×10^{-6} M of the equilibrium binding constant ($K_d=k_d/k_a$), cynarin has an ability to replace CD80 to bind to the CD28 since its binding constant is about 1.7×10^{-7} M. The SPR binding experiments show further evidence that cynarin can compete for the CD28 binding site for CD80, since the binding capacity of CD80 is largely reduced in the presence of cynarin. Further NMR experiments need to be done to elucidate more detail of the binding between CD28 and cynarin, and to describe the 3D structure of the CD28/cynarin complex.

ACKNOWLEDGEMENTS

This work was partially supported by the National Science Council, Taiwan, R.O.C. (NSC 96-2320-B-001-022-MY3). We thank Prof. Lou-Sing Kan of the Institute of Chemistry, Academia Sinica, for access to the Biocore 3000 instrument.

REFERENCES

1. O. Acuto, and F. Michel. CD28-mediated co-stimulation: a quantitative support for TCR signalling. *Nat Rev Immunol.* **3**:939–951 (2003) doi:10.1038/nri1248.
2. J. P. Allison. CD28-B7 interactions in T-cell activation. *Curr Opin Immunol.* **6**:414–419 (1994) doi:10.1016/0952-7915(94)90120-1.
3. C. H. June, J. A. Ledbetter, P. S. Linsley, and C. B. Thompson. Role of the CD28 receptor in T-cell activation. *Immunol Today.* **11**:211–216 (1990) doi:10.1016/0167-5699(90)90085-N.
4. A. H. Sharpe, and G. J. Freeman. The B7-CD28 superfamily. *Nat Rev Immunol.* **2**:116–126 (2002) doi:10.1038/nri727.
5. E. Akalin. Immunosuppression minimization protocols: how should they be monitored? *Nat Clin Pract Nephrol.* **4**:484–485 (2008) doi:10.1038/ncpneph0910.
6. M. Veroux, D. Corona, G. Giuffrida, M. Gagliano, M. Sorbello, C. Virgilio, T. Tallarita, D. Zerbo, A. Giaquinta, P. Fiamingo, M. Macarone, G.L. Volti, P. Caglia, and P. Veroux. New-onset diabetes mellitus after kidney transplantation: The role of immunosuppression. *Transplant Proc.* **40**:1885–1887 (2008) doi:10.1016/j.transproceed.2008.06.005.
7. G. C. Dong, P. H. Chuang, M. D. Forrest, Y. C. Lin, and H. M. Chen. Immuno-suppressive effect of blocking the CD28 signaling pathway in T-cells by an active component of Echinacea found by a novel pharmaceutical screening method. *J Med Chem.* **49**:1845–1854 (2006) doi:10.1021/jm0509039.
8. A. W. Schuttelkopf, and D. M. van Aalten. PRODRG: a tool for high-throughput crystallography of protein–ligand complexes. *Acta Crystallogr D Biol Crystallogr.* **60**:1355–1363 (2004) doi:10.1107/S0907444904011679.
9. G. M. Morris, D. S. Goodsell, R. S. Halliday, R. Huey, W. E. Hart, R. K. Belew, and A. J. Olson. Automated docking using a Lamarckian genetic algorithm and an empirical binding free energy function. *J Comput Chem.* **19**:1639–1662 (1998) doi:10.1002/(SICI)1096-987X(19981115)19:14<1639::AID-JCC10>3.0.CO;2-B
10. W. Humphrey, A. Dalke, and K. Schulten. VMD: visual molecular dynamics. *J Mol Graph.* **14**:33–38 (1996) doi:10.1016/0263-7855(96)00018-5.
11. W. DeLano. *The PyMOL User's Manual*. USA DeLano Scientific, San Carlos, CA, 2002.
12. C. Hetenyi, and D. van der Spoel. Efficient docking of peptides to proteins without prior knowledge of the binding site. *Protein Sci.* **11**:1729–1737 (2002) doi:10.1110/ps.0202302.
13. E. J. Evans, R. M. Esnouf, R. Manso-Sancho, R. J. Gilbert, J. R. James, C. Yu, J. A. Fennelly, C. Vowles, T. Hanke, B. Walse, T. Hunig, P. Sorensen, D. I. Stuart, and S. J. Davis. Crystal structure of a soluble CD28-Fab complex. *Nat Immunol.* **6**:271–279 (2005) doi:10.1038/ni1170.
14. F. Luhder, Y. Huang, K.M. Dennehy, C. Guntermann, I. Muller, E. Winkler, T. Kerkau, S. Ikemizu, S. J. Davis, T. Hanke, and T. Hunig. Topological requirements and signaling properties of T cell-activating, anti-CD28 antibody superagonists. *J Exp Med.* **197**:955–966 (2003).